



AN INVESTIGATION ON DYNAMIC BEHAVIOR AND CHARACTERISTICS OF SHARIF UNIVERSITY OF TECHNOLOGY SHAKING TABLE (SST)

Hassan MOGHADDAM¹, Khashayar FARZANIAN², Ehsan TAHERI³

ABSTRACT

This paper presents the results of an analytical and experimental study on the dynamic characteristics of the Sharif University of Technology Shaking Table (SST). This 3 degree of freedom shaking table is driven by servo-hydraulic actuators, and consist of a 12 ton, 4×4×0.6_m steel deck. The main objective of this investigation is to calculate the oil column resonance frequency (OCRF) and determining mechanical model of SST. The results of tests and FRF method are used to evaluate the OCRF. An analytical model was developed for analyzing the dynamic behavior of SST. This model takes into account the mechanical components of SST. This model enables us to determine the forces mobilized in the deck due to various sources including the inertial, dissipative and elastic resistance forces. An identification approach is used based on the measured hysteresis response to determine the fundamental model parameters. This includes the effective horizontal mass, effective horizontal stiffness, and the coefficients of the classical Coulomb friction and viscous damping elements which represent the dissipative forces. It is shown that the model can comprehensively represent the mechanical, hydraulic and electronic characteristics of the shaking table. Thus, this mathematical model can be used for simulating the dynamic response of the shake table subjected to given excitations with acceptable accuracy.

INTRODUCTION

OBJECTIVES OF STUDY

Theoretical and experimental researches in earthquake engineering are mostly verified by tests on shaking tables, which the accuracy of their results is of great importance. These results might be unreliable as it is observed in the last century that the results driven from shaking table tests had errors and deficiencies.

The primary shaking tables were excited by man power which were only used to demonstrate the qualitative seismic behaviour of structures. Engineering science development during 20th century resulted in the utilization of electrical power and eventually servo-controlled hydraulic actuators instead. During these developments the degrees of freedom of shaking tables increased from one to six degrees. These developments produced a great evolution in civil engineering sciences.

¹ Professor, Sharif University of Technology, Tehran, Iran, moghadam@sharif.edu

² MSc Student, Sharif University of Technology, Tehran, Iran, kh.farzanian@yahoo.com

³ MSc Student, Sharif University of Technology, Tehran, Iran, ehn.taheri@yahoo.com

Shaking tables are consisted of three fundamental sections: electronic, hydraulic, and mechanical. Each of these three sections are made up of various components (Fig.1). The dynamic behaviour and characteristics of mechanical system of shaking tables is complicated because of the interaction between these various components.

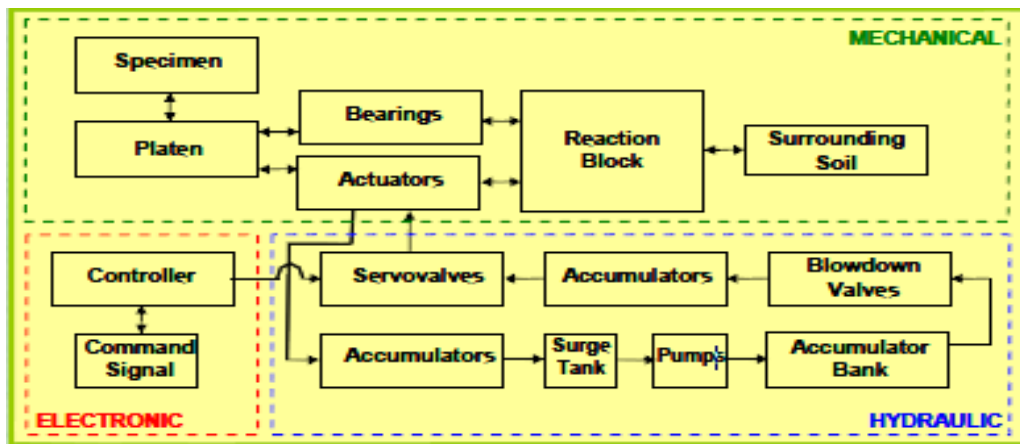


Figure 1. Interactions between all components of shaking table

Obtaining the dynamic model of shaking table and identifying its characteristics helps to have a more precise understanding of shaking table behavior. In fact shaking table dynamic identification is necessary. In this paper this dynamic identification of SST is determined.

OVERVIEW OF SST

3 degree of freedom SST is excited by 3 hydraulic actuators in 2 horizontal directions which also has the ability to rotate around vertical axis. These hydraulic actuators have 250L/min pumping capacity, hydraulic pressure of actuator chamber is 280bar, 1300L oil chamber capacity, and full chamber weight is 4.3ton .its control system is one-variable controller (OVC) in which displacement is the variable. SST deck is a 4m×4m×0.6m steel box with top, bottom and side 25mm thick plates. Seven 6cm thick joint stiffeners with rigid behavior are located at the end of each of the 3 hydraulic actuators and 4 hold-down struts. 2cm thick stiffeners are designed perpendicular to the rigid joint stiffeners in order to transfer the displacement uniformly and prevent punching of the side and bottom plates. 0.8m×0.8m mesh of vertical 2cm thick stiffeners is designed to increase rigidity of the top and bottom plates of SST. It is expected that this steel deck present a rigid behavior under extreme dynamic loading, but in fact this is not totally fulfilled. The details of SST steel deck and its three hydraulic actuators are illustrated in Fig.2.



Figure 2. SST steel deck view consist of 3 hydraulic actuators

OIL COLUMN RESONANCE (OCR)

In most shaking tables, oil column resonance frequencies (OCR) stand in the range of earthquake frequencies (0_{Hz} to 15_{Hz}). This occurrence causes noises which lead to errors in test results. By utilizing analytical method OCRF was determined for SST and the result was verified by frequency response function method (FRF) and experimental results.

ANALYTICAL MODEL OF OCR

Hydraulic actuators exert dynamic load utilizing internal pistons driven by high oil hydraulic pressure which performs like a mass-oil column system model. When the test system has a mass coupled to the actuator, it sits on the column of oil. Since oil has a finite stiffness, it has a resonance. If the mass is high enough, and the oil column is large, the resonance can creep into the control band. Delta-P compensation helps to tame this resonance. It is good practice to use delta-P for all systems where a free mass is coupled to the actuator. Using Eq.(2) oil column resonance for the system would be calculated analytically.

$$f = \frac{\omega}{2\pi} \quad \omega = \sqrt{\frac{K}{M}} \quad K_{oil} = \frac{2\beta A}{L} \quad (1)$$

By utilizing Eq.(2) and according to Fig.3 final equations for OCRF are obtained (Eq. (3)).

$$f_{oil} = \frac{1}{2\pi} \sqrt{\frac{2\beta A}{LM}} \quad f_{oil} = \frac{1}{2\pi} \sqrt{\frac{2\beta A^2}{VM}} \quad (2)$$

In which effective bulk modulus β , SST mass M (including: test specimen, steel deck, and moving components of shaking table attached to the steel deck), piston area A, oil column length L, and total oil volume V. OCRF calculated for SST by analytical equation presented above equals 28.6Hz.

FREQUENCY RESPONSE FUNCTION (FRF)

Different systems respond differently to various frequencies. Some systems increase or decrease components of certain frequencies. The method that relates the output to the input of the system for various frequencies is system frequency response. Frequency response is the relationship between system input and output in Fourier domain. In systems: system input $X_{(j\omega)}$, system output $Y_{(j\omega)}$ and frequency response $H_{(j\omega)}$ (each in frequency domain) are indicated in Fig.3 and Eq.(1).

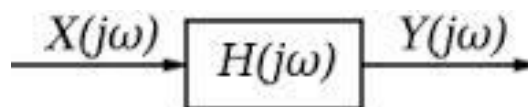


Figure 3. FRF

$$Y_{(j\omega)} = H_{(j\omega)} X_{(j\omega)} \quad ; \quad \frac{Y_{(j\omega)}}{X_{(j\omega)}} = H_{(j\omega)} \quad (3)$$

By utilizing FRF method and input and output data of an experiment (Zarand earthquake experiment on SST) $H(j\omega)$ function would be obtained and by defining the first sudden jump point in the diagram the resonance frequency domain would be specified. By exploiting the data from 5 accelerometer, 3 set of input and output data in each horizontal direction was provided and based on these diagrams OCRF was determined. Defined ω for each data set of accelerometers was in the range of $175_{\text{rad/sec}}$ to $180_{\text{rad/sec}}$ as illustrated in Fig.4. According to Eq.(1) $f_{\text{oil}}=28.3_{\text{Hz}}$, which in accordance with analytical results. Since earthquake frequencies are mostly in the range of 0_{Hz} to 15_{Hz} the defined OCRF for SST is desirable. As the OCRF was determined for a SST test which was designed for almost full weigh capacity (25_{ton}) so the results are reliable, because lighter test specimens generate higher OCRF. Considering prevention of frequency interference, these results testify reliable performance of SST.

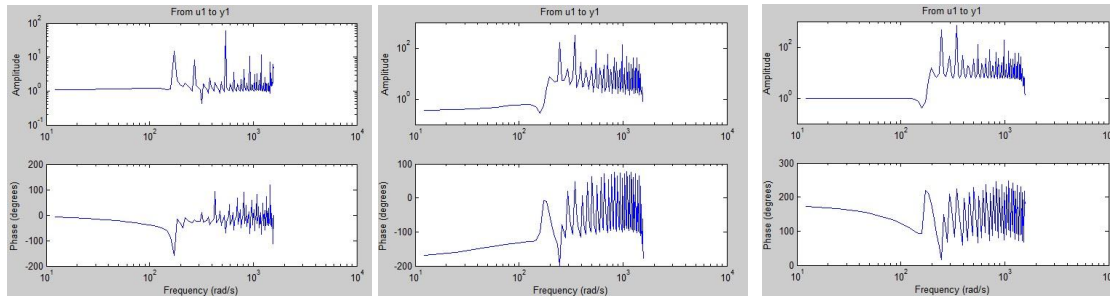


Figure 4. Oil column resonance frequency of SST

THE ANALYTICAL MODEL OF SST MECHANICAL SYSTEM

SHAKING TABLE MECHANICAL COMPONENTS

The forces exerted on the steel deck by the hydraulic actuators are balanced by:

- (1) The inertia force due the mass of the steel deck, hold-down struts and moving parts of the hydraulic actuators.
- (2) The elastic restoring force due to the nitrogen pressure inside the inclined hold-down struts.
- (3) The Coulomb-type dissipative forces due to (a) sliding of the steel deck on the vertical and lateral bearings, (b) rotation of hinges (swivels) at both ends of the hold-down struts, and (c) sliding of the hydraulic actuator arm and piston inside each of the two hydraulic actuators.
- (4) the viscous-type dissipative forces due to various sources, such as (a) oil film between the wear plates and the vertical and lateral bearings, (b) air flow in and out of the hold-down struts, and (c) cross-port leakage in the horizontal actuators, which accounts for the damping within the actuators.

CONCEPTUAL SST MODEL AND ITS DYNAMIC EQUATIONS

For the first estimation, the steel deck is considered as a rigid body with the mass of M_{sd} subjected to displacement u_x along x-axis. The four vertical bearings and the six lateral bearings are treated as dissipative components with Coulomb friction and viscous damping. The hold-down struts correspond to the system inertial, elastic, and dissipative forces. The equation of motion for SST mechanical system can be written as

$$F_I(t) + F_E(t) + F_D(t) = F_A(t) \quad (4)$$

where $F_A(t)$ is the resultant horizontal longitudinal force from both actuators, and FI , FE , and FD are the inertia, elastic, and damping forces, respectively. These forces can be expressed as

$$F_I = M_e \ddot{u}_x + 4\bar{M}_e' \left(\frac{u_x}{h} \right)^2 \ddot{u}_x + 4\bar{M}_e' \left(\frac{\dot{u}_x}{h} \right)^2 u_x \quad (5)$$

$$F_E = K_e u_x + k_e' \left(\frac{u_x}{h} \right)^2 u_x \quad (6)$$

$$F_D = \left[F_\mu + C_e |\dot{u}_x|^\alpha + 2C_\beta \left| \frac{u_x}{h} \right|^{1+\beta} |\dot{u}_x|^\beta + \mu_e^{(iv)} F_{hd} \left(\frac{u_x}{h} \right)^2 \right] \text{sign} \dot{u}_x \quad (7)$$

EFFECTIVE MASS

Effective mass parameter presented in Eq.(5) is estimated as

$$M_e = M_{sd} + M_{ha} + 4\bar{M}_e', \quad \bar{M}_e' = \frac{1}{3} m_a \left(\frac{l_o}{h} \right)^2 + \frac{1}{3} m_b$$

$$\bar{M}_e' = \frac{1}{2} \left[\frac{5}{3} m_b - \frac{4}{3} m_a \left(\frac{l_o}{h} \right)^2 \right] \quad (8)$$

where M_{sd} is the mass of the steel deck; M_{ha} is the total mass of each of the three hydraulic actuators moving parts; M_a and M_b are the masses of the piston and cylinder of one hold-down strut, respectively; and l_o and h are the corresponding lengths.

The second term in Eq.(5) amounts to less than 1% of the first term, and can be ignored (because of the small term of $\left(\frac{u_x}{h} \right)$, the amount of this term squared is negligible in comparison to the first term of equation). The last term in Eq.(5) is also negligible. Thus, only the first term in Eq.(5) is significant. 5% of the mass M_{sd} of the steel deck.

EFFECTIVE HORIZONTAL STIFFNESS BECAUSE OF HOLD-DOWN STRUTS

To obtain effective stiffness, it should be assumed as adiabatic condition. So it is possible to utilize following equations to achieve effective stiffness which is used in Eq.(6)

$$K_e = \frac{4P_o A}{h}, \quad K_e' = \frac{1}{2} \left(\frac{\gamma h}{l_o} - 1 \right) K_e \quad (9)$$

where p_o is the initial pressure inside the hold-down strut, A is the cross-section area of the strut cylinder, h is the (fixed) height from pin-to-pin of the hold-down strut in its initial configuration ($u_x=0$), l_o is the initial length of the piston, and γ is the gas constant which fulfilled the hold-down strut. For the hold-down struts of the SST, $h=1.2\text{m}$, $l_o=0.8\text{m}$, $\gamma=1.44$, and $u_x \leq 0.5\text{m}$. In this case, the

ratio $\bar{k}_e'(\mathbf{u}_x/h)^2/\bar{k}_e$ amounts to less than 3%. Therefore, the relative contribution of the nonlinear elastic restoring force term is small and can be neglected in most cases.

EFFECTIVE LATERAL DISSIPATIVE FORCES

The first term in Eq.(9) corresponds to the Coulomb frictional force given by

$$F_\mu = \mu_e' F_{hd} + \mu_e'' F_{sd+ha} + \mu_e''' F_t, \quad \mu_e' = \mu_e'' + 4\mu_{hg} K \left(\frac{a}{h} \right) \quad (10)$$

where $F_{hd} = 4p_0A$ is the initial vertical force due to pre-charge nitrogen pressure in the hold-down struts, F_{sd+ha} is the combined weight of the steel deck and part of the actuators supported by the vertical bearings; F_t is the time dependent total normal force on the lateral bearings; μ_e'' and μ_e''' are the Coulomb friction coefficients on the vertical and lateral bearings, respectively; μ_{hg} is the Coulomb friction coefficient in the swivels of the hold-down struts; a is the radius of the hinge and K is a constant that depends on the distribution of forces on the hinge. The second term in Eq.(7) represents viscous damping in the actuators in which C_e is an effective viscous damping constant and $0 \leq \alpha \leq 1$. The third term in Eq.(7) represents viscous damping in the hold-down struts with $0 \leq \beta \leq 1$. Finally, the last term in Eq.(7) is a nonlinear term involving friction on the hinges of the hold-down struts. In that term.

$$\mu_e^{(iv)} = 4\mu_{hg} K \left(\frac{a}{h} \right) \frac{\gamma}{2} \left(\frac{h}{\lambda_o} \right) \quad (11)$$

PARAMETER ESTIMATION BY ANALYSIS OF HYSTERESIS LOOPS

In this section, the hysteresis loops relating actuator force to displacement, velocity, or acceleration of the table during periodic triangular or sinusoidal tests will be used to determine the most important characteristics of the shake table mechanical system. The basic conceptual model of the system, inspired in part by Eq.(4) to Eq.(7), is expressed by

$$M_e(u_x) \ddot{u}_x(t) + F_E(u_x) + F_o(\dot{u}_x) = F_A(t) \quad (12)$$

where $u_x(t)$ is the horizontal longitudinal total displacement of the steel deck, M_e is the effective mass, and F_E , F_D , and F_A are the total elastic, dissipative, and actuator forces, respectively. It is assumed that $M_e(u_x)$ is an even function of u_x , and that $F_E(u_x)$ and $F_D(\dot{u}_x)$ are odd functions of u_x and \dot{u}_x , respectively. The simplified model given by Eq.(9) excludes dependence of F_E and F_D on the history of u_x and \dot{u}_x , and ignores certain possible inertial and dissipative terms that depend on products of u_x and \dot{u}_x .

The data from periodic tests were low-pass filtered, except where noted, with a cut-off frequency of four times the fundamental frequency of the test in an attempt to keep the first few harmonics of the potentially nonlinear response while filtering out higher frequencies. To ensure that the steady-state response had been reached, the analysis of the response was based on the second to the last cycle of each test. Finally, in the case of the triangular tests, only the portions of the time histories over which constant velocities had been reached were used in the identification procedure.

Unfortunately, the data experiments for triangular tests were not accessible, so we have used some sinusoidal tests instead of triangular tests to achieve the effective parameters. Obviously this estimation affects the accuracy of parameter results, but by using modified sinusoidal tests which has the most similarity to triangular shape graph of data tests, these errors become negligible.

The identification approach used here takes advantage of the periodic nature of $u_x(t)$, $\dot{u}_x(t)$, and $\ddot{u}_x(t)$ during a test cycle ($0 < t < T$). Selecting the cycle of test data so that the displacement $u_x(t)$ is positive over the first half ($0 < t < T/2$) of the cycle; the following time instants t_1 , t_2 , t_3 , and t_4 are considered: $0 < t_1 < T/4$, $t_2 = T/2 - t_1$, $t_3 = T/2 + t_1$, and $t_4 = T - t_1$. With this notation, the periodicity leads to

$$\begin{aligned} u_x(t_2) &= u_x(t_1), \dot{u}_x(t_2) = -\dot{u}_x(t_1), \ddot{u}_x(t_2) = \ddot{u}_x(t_1) \\ u_x(t_4) &= u_x(t_3), \dot{u}_x(t_4) = -\dot{u}_x(t_3), \ddot{u}_x(t_4) = \ddot{u}_x(t_3) \end{aligned} \quad (11)$$

$$\begin{aligned} u_x(t_4) &= -u_x(t_1), \dot{u}_x(t_4) = \dot{u}_x(t_1), \ddot{u}_x(t_4) = -\ddot{u}_x(t_1) \\ u_x(t_3) &= -u_x(t_2), \dot{u}_x(t_3) = \dot{u}_x(t_2), \ddot{u}_x(t_3) = -\ddot{u}_x(t_2) \end{aligned} \quad (12)$$

Applying Eq.(9) at times t_1 and t_2 , t_3 and t_4 , t_1 and t_4 , and t_2 and t_3 leads to

$$M_e(u_x(t_1))\ddot{u}_x(t_1) + F_E(u_x(t_1)) = [F_A(t_1) + F_A(t_2)]/2 \quad (13)$$

$$M_e(u_x(t_3))\ddot{u}_x(t_3) + F_E(u_x(t_3)) = [F_A(t_3) + F_A(t_4)]/2 \quad (14)$$

$$F_D(\dot{u}_x(t_1)) = [F_A(t_1) + F_A(t_4)]/2 \quad (15)$$

$$F_D(\dot{u}_x(t_2)) = [F_A(t_2) + F_A(t_3)]/2 \quad (16)$$

Eq.(14) and Eq.(15) indicate that the dissipative forces can be obtained directly from the data. On the other hand, Eq.(12) and Eq.(13) indicate that additional considerations need to be made to separate the inertial and elastic forces.

ESTIMATION OF ELASTIC FORCES AND EFFECTIVE HORIZONTAL STIFFNESS

To separate the elastic forces from the inertial and dissipative forces, the results of the periodic triangular tests, in which the horizontal acceleration \ddot{u}_x of the platen is zero for intervals of time are used. In this case, Eq.(12) and Eq.(13) reduce to

$$F_E(\bar{u}_x(t_1)) = \frac{1}{2} [F_A(t) + F_A(T/2 - t)]/2 \quad (17)$$

$$\bar{u}_x(t) = \frac{1}{2} [u_x(t) + u_x(T/2 - t)]/2 \quad (0 < t < T/4) \quad (18)$$

and

$$F_E(\bar{u}_x(t_1)) = \frac{1}{2} [F_A(t) + F_A(3T/2 - t)]/2 \quad (19)$$

$$\bar{u}_x(t) = \frac{1}{2} [u_x(t) + u_x(3T/2 - t)]/2 \quad (T/2 < t < 3T/4) \quad (20)$$

which provide estimates of $F_E(u_x)$ for $u_x > 0$ and $u_x < 0$, respectively.

As it was indicated previously, K_e can be obtained from Eq.(9) theoretically.

Finally, the theoretical equations of motion presented in Section 2 indicate that the total non-dissipative force for $\ddot{u}_x = 0$ can be expressed by

$$K_e u_x + K'_e (u_x/h)^2 u_x + 2\bar{M}'_e (\dot{u}_x/h)^2 u_x \quad (21)$$

where K_e , K'_e , and M_e are given by Eq.(8) and Eq.(9). The second cubic term in this equation is negligible compared with the first term (verified by estimated computations). The third term is an inertial term associated with the rotation of hold-down struts. For more simplification periodic triangular data results were used again since in \dot{u}_x (derivative of displacement) is constant so $2\bar{M}'_e(\dot{u}_x/h)^2 u_x$ can be added to K_e and the whole equation would be

$$\left[K_e + 2\bar{M}'_e(\dot{u}_x/h)^2 \right] u_x \quad (22)$$

ESTIMATION OF EFFECTIVE MASS

By using Eq.(17) and Eq.(18) and regarding $\bar{u}_x(t) = \frac{1}{2}[u_x(t) + u_x(T/2-t)]/2$ for ($0 < t < T/4$) and $\bar{u}_x(t) = \frac{1}{2}[u_x(t) + u_x(3T/2-t)]/2$ for ($T/2 < t < 3T/4$) and also $F_E(u_x) = K_e u_x$ mentioned in previous parts the equation for estimating effective mass $M_e(u_x)$ would be

$$\begin{aligned} M_e(\bar{u}_x(t)) \ddot{\bar{u}}_x(t) &= \frac{1}{2}[F_A(t) - K_e u_x(t)] + \frac{1}{2}[F_A(T/2-t) - K_e u_x(T/2-t)] \\ \ddot{\bar{u}}_x(t) &= \frac{1}{2}[\ddot{u}_x(t) + \ddot{u}_x(T/2-t)] \quad , \quad (0 < t < T/4) \end{aligned} \quad (23)$$

for $\ddot{u}_x > 0$, and

$$\begin{aligned} M_e(\bar{u}_x(t)) \ddot{\bar{u}}_x(t) &= \frac{1}{2}[F_A(t) - K_e u_x(t)] + 1/2[F_A(3T/2-t) - K_e u_x(3T/2-t)] \\ \ddot{\bar{u}}_x(t) &= \frac{1}{2}[\ddot{u}_x(t) + \ddot{u}_x(3T/2-t)] \quad , \quad (T/2 < t < 3T/4) \end{aligned} \quad (24)$$

for $\ddot{u}_x < 0$.

Utilizing Eq.(22) and Eq.(23) and obtained K_e in the last section the SST effective mass could be estimated. To calculate μ_e , data results of $u_x(t)$, $\dot{u}_x(t)$, and F_A from sinusoidal test series with different frequencies, domains, and accelerations (test parameters) were used. It is notable to point out that more data results with various frequencies, domains, and accelerations leads to more accuracy in estimation of μ_e , and M_e . In fact this investigation indicates that spectral test parameters leads to more accurate results than discrete parameters.

ESTIMATION OF THE EFFECTIVE TOTAL DISSIPATIVE FORCE

Eq.(14) and Eq.(15) are used here to separate the total dissipative forces from the inertial and elastic components of the total actuator force. In particular, the dependence of the total dissipative forces on velocity is given by

$$\begin{aligned} F_D(\dot{u}_x(t)) &= [F_A(t) + F_A(T-t)]/2 \\ \dot{u}(t) &= [\dot{u}_x(t) + \dot{u}_x(T-t)]/2 \end{aligned} \quad (25)$$

with $0 < t < T/4$ for $\dot{u}_x > 0$, and $T/4 < t < T/2$ $\dot{u}_x < 0$.

Recording total motivation force during tests is also needed (it is notable to consider that these section tests are also sinusoidal, not triangular periodic with constant \dot{u}_x). It should be considered that total motivation force magnitude jumps in the moment which the shaking table steel deck motion direction reverses. In the previous studies the reasons of this jump is not mentioned. But regarding the analysis in this investigation and considering SST analytical model and the difference between maximum static frictional force and kinetic frictional force, the main reason for this difference is transformation of these two types of frictional forces. In fact the maximum static frictional force in the moment the motion starts is more than constant kinetic frictional force during dynamic motion which might cause this jump. To eliminate these errors a filter with cut-off frequency should be used with a frequency more than specimen frequency and less than OCRF obtained in section 2.

To obtain dynamic characteristics of SST mechanical system, C_e (effective dissipation coefficient) could be calculated by utilizing Eq.(24), but to achieve this sinusoidal tests is required.

Static friction varies from 0 to its maximum amount before the motion starts, which during this immobility \dot{u}_x is 0, but frictional dissipative force still exists because the resistance force is neither corresponds to inertial force (\ddot{u}_x) nor elastic force (u_x) hence the term F_D in motion equation could be presented as in Eq.(25).

$$F_D(t) = F_{\mu e} + C_e |\dot{u}_x(t)|^\alpha \quad (25)$$

$F_{\mu e}$ in Eq.25 corresponds to coulomb frictional force and C_e is viscose friction coefficient. Utilizing sinusoidal test series and given equations α , C_e , and $F_{\mu e}$.

Would be calculated. Regarding Eq.(25) it is important that this equation only gives the absolute amount of F_D so the sign and direction of this force is defined based on the velocity as in Eq.(26).

$$F_D(t) = \left(F_{\mu e} + C_e |\dot{u}_x(t)|^\alpha \right) \text{sign}(\dot{u}_x(t)) \quad (26)$$

SST ANALYTICAL MODEL

Considering mentioned equations in previous sections the procedure of obtaining the parameters and effective coefficients of SST motion equation was presented. In this investigation the formulation and the calculation method of parameters and coefficients, techniques to compute these coefficients and types of tests are explained. Finally, SST motion equation is presented:

$$F_A(t) = M_e \ddot{u}_x(t) + K_e u_x(t) + \left(C_e |\dot{u}_x(t)|^\alpha + F_{\mu e} \right) \text{sign}(\dot{u}_x(t)) \quad (27)$$

Where M_e is the effective mass, K_e is the effective stiffness, C_e is the effective dissipation coefficient, and $F_{\mu e}$ is coulomb frictional force. Also $u_x(t)$, $\dot{u}_x(t)$, and $\ddot{u}_x(t)$ are SST steel deck displacement, velocity, and acceleration respectively. Fig.5 illustrates the SST conceptual dynamic model.

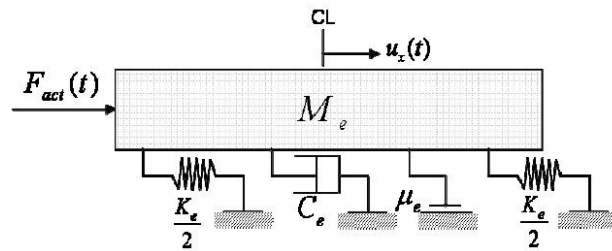


Figure 5. SST conceptual dynamic model

CONCLUSION

Based on test results OCRF was defined (28.3 Hz) which indicates the desirable performance of SST in usual frequencies of earthquakes (0 to 15 Hz). Defining OCRF is essential for test experiments with limited scale specimens in which the earth quake frequency increases. Utilizing dampers in order to increase OCRF is necessary in case of SST OCRF being in the domain of test earth quake frequency to achieve more accurate results, otherwise test results should be filtered around OCRF.

By utilizing test experiment results and a mathematical model for the mechanical components of SST, a dynamic conceptual model of SST was provided. The accuracy of test results was enhanced by increasing test numbers. In mathematical model for the mechanical components of SST nonlinear terms were developed. These terms were investigated by numerical computations and analytical calculations and were not considered in case of being negligible. Finally the conceptual dynamic model for mechanical system of SST with $M_e = 13.2$ ton, $K_e = 0.72$ MN/m, $C_e = 29.6$ KN/(m/s)^{1/2}, and $\mu_e = 1.27\%$ was developed.

REFERENCES

- Ozcelik, O., Luco, J.E., Conte J.P., Trombetti T.L. and Restrepo J.I. *Experimental characterization, modeling and identification of the NEES-UCSD shake table mechanical system*. Earthquake Engineering and Structural Dynamics, 2008.
- Clough RW and Penzien J (1993) *Dynamics of Structures*, 2nd Ed., McGraw-Hill Book Company, New York
- Vu D (2002) *Strength properties of metakaolin blended concrete*, Ph.D. Thesis, Delft Technical University of Technology, The Netherlands
- Rinawi AM, Clough RW. Shaking table–structure interaction. EERC Report No. 91/13, Earthquake Engineering Research Center, University of California at Berkeley, CA, 1991.
- Conte JP, Trombetti TL. Linear dynamic modeling of a uni-axial servo-hydraulic shaking table system. *Earthquake Engineering and Structural Dynamics* 2000; 29(9):1375–1404.
- Crewe AJ, Severn RT. The European Collaborative Programme on evaluating the performance of shaking tables. *Philosophical Transactions of the Royal Society of London Series A* 2001; 359:1671–1696.
- Hwang JS, Chang KC, Lee GC. The system characteristics and performance of a shaking table. NCEER Report No. 87-0004, National Center for Earthquake Engineering Research, State University of New York at Buffalo, NY, 1987.